Bull Earthquake Eng
DOI 10.1007/s10518-015-9747-9

ORIGINAL RESEARCH PAPER

# Seismic vulnerability of building aggregates through hybrid and indirect assessment techniques

**Rui Maio[1] · Romeu Vicente[1] · Antonio Formisano[2] · Humberto Varum[3]**

Received: 23 May 2014 / Accepted: 11 March 2015


**Abstract** This work approaches the seismic vulnerability assessment of an old stone masonry building aggregate, located in *San Pio delle Camere* (*Abruzzo*, Italy), slightly affected by the 2009 April 6th earthquake occurred in *L'Aquila* and its districts. This building aggregate has been modelled by using the 3muri® software for seismic analysis of masonry constructions. On one hand, static non-linear numerical analyses were performed to obtain capacity curves together with the prediction of damage distributions for the input seismic action (hybrid technique). On the other hand, indirect techniques, based on different vulnerability index formulations, were used for assessing the building aggregate's behaviour under earthquake action. The activities carried out have provided a clear framework on the seismic vulnerability of building aggregates, as well as aid future retrofitting interventions.

**Keywords** Seismic vulnerability · Building aggregates · Macro-elements · Fragility curves · Damage distributions · Vulnerability index

✉ Rui Maio
ruiamaio@ua.pt

Romeu Vicente
romvic@ua.pt

Antonio Formisano
antoform@unina.it

Humberto Varum
hvarum@fe.up.pt

[1] Department of Civil Engineering, University of Aveiro, Campus Universitário de Santiago, 3810-193 Aveiro, Portugal

[2] Department of Structures for Engineering and Architecture, University of Naples Federico II, P.le Tecchio 80, 80125 Naples, Italy

[3] Department of Civil Engineering, Faculty of Engineering, University of Porto, R. Dr. Roberto Frias, s/n, 4200-465 Porto, Portugal

Published online: 22 March 2015

## 1 Introduction

Earthquakes are one of the most frightening, destructive and deadliest natural disasters ever known to human kind. History has shown that Mediterranean bordering countries are the most vulnerable seismic areas in Europe. Following the XVIII Century the most two relevant seismic events, in terms of fatalities, were the 1st November 1755 Lisbon, Portugal, and the 28th December 1908 Messina, Italy.

The damage caused by earthquakes depends not only on the intensity but also on the vulnerability of structures. In Portugal and Italy, a great part of the building stock was not subjected to specific seismic design and old buildings need rehabilitation interventions. Moreover, in historical city centres these buildings were weakened due to economical interests, in which for example, load bearing walls at the ground floor level were excessively intervened with more and larger openings, reducing the shear strength of those walls and subsequently of the whole building.

Presently, in historical centres, it is very difficult to analyse a building as an independent structure when, for example, it shares the same boundary walls, emerging this way the need to assess building aggregates. Generally, building aggregates are conditioned to urban diachronic construction process. The structural units constituting the aggregate interact amongst themselves under seismic action, giving the aggregate different characteristics from the individual building unit. Over the years, this transformation process of the historical centres raised the need for specific structural analysis to these particular structures. The building aggregate’s response to a seismic action is naturally associated to distinct factors, such as the confinement, the quality of the connections between adjacent buildings and, obviously, factors regarding the inherent mechanical properties of each structure, where the span between walls, the connection between floors and walls, the roofing system and both in-height and in-plan irregularities are considered (Vicente 2008).

Moreover, the Portuguese and Italian historical centres, once overpopulated, are nowadays in need of structural rehabilitation to bring them back to life again. Thus, in recent years several authors have focused attention on historical city centres in prone seismic areas, where the most vulnerable buildings are concentrated. This activity is framed into a more general context, where scientists, civil protection, stakeholders and other responsible authorities must give their best to reduce the repercussions of future devastating earthquakes.

On the one hand, as large-scale assessment methodologies are mainly based on basic observational data for a significant number of buildings and are strictly focused on individual buildings assessment, the collected data regarding the behaviour of building aggregates, such as the interactions and connections between adjacent buildings, is practically inexistent. On the other hand, assessment methodologies at the individual building scale, such as numerical analysis, are generally more time consuming and require several additional detailed data. Moreover, due to computational and modelling issues, on these individualised assessment scales, the previously mentioned interactions between adjacent buildings are usually not considered, as they involve additional computational efforts. Hence, a new and validated methodology suitable for a middle-term assessment methodology is needed for the seismic vulnerability assessment of building aggregates.

## 2 Literature review

Masonry buildings remain as one of the most common building typology and one of the most vulnerable too. In Europe, over recent years, the trend is to establish a simplified mechanical approach for the seismic vulnerability assessment of masonry buildings, using procedures based on non-linear static analyses and on the Capacity Spectrum Method, CSM (Freeman 1998).

Nevertheless, during the past 30 years several methodologies have been developed in order to assess the seismic vulnerability both for individual and aggregate buildings (Calvi et al. 2006). The extensive research developed by these authors led to the discussion of the advantages and disadvantages of various current procedures in order to find guidelines for a hypothetical optimal methodology.

Past European research projects funded by the European Commission dealing with seismic risk and loss estimation (Mouroux and Le Brun 2006; Erdik 2007) are consensual in dividing these methodologies in three main groups, accordingly to the scale defined in each assessment project. Recently, Chever (2012) summarised the most used methodologies all over the world for the seismic vulnerability assessment of buildings, cataloguing them by the analysis scale, from thousands of buildings, few dozens to few hundred and to individual buildings. In this paper, different analysis scale methodologies were used for the assessment of a building aggregate.

However, independently from investigation method used in order to make possible the seismic vulnerability assessment of buildings, it is fundamental to have the knowledge over the structures studied. The level of knowledge clearly influences the engineer's way of facing seismic vulnerability assessment. Thus, different methodologies can be chosen according to the quantity and quality of the building survey. To achieve a thorough knowledge of the building aggregate, a joint working group formed by ReLUIS, the Italian Civil Protection Department and other stakeholders has established absolutely crucial an approach on the following features: the formation and evolution of the aggregate itself; the morphological characteristics of the site and environmental context in which the aggregate is located; the typologies of buildings and their variation during the evolution process; the analysis of the constructive technique and its workmanship application. Based on the building knowledge process, different approaches have been developed for seismic behaviour evaluation of masonry building aggregates (Maio 2013; Formisano et al. 2013).

## 3 San Pio delle Camere

*San Pio delle Camere* is a small medieval village born in 1001 in the region of *Abruzzo*, about 25 km south from *L'Aquila*, 800 meters above the sea level. Recently included in the European Cultural Heritage Protection Program, *its* historical centre is located in the upper part of the village, as most of the medieval Italian villages and was built along the main axis that crosses the entire village, *Via del Protettore*. Buildings along this street are generally narrow, featuring low ceiling height and often showing in-height irregularities. During the last Century, several intrusive interventions were carried out, mischaracterising both the architecture and morphology of the village.

The generalised characteristic of historical centres layout is the structural continuity of buildings (Carocci 2001), frequently ensured when adjacent buildings, structurally connected to each other, are capable to induce either constraint vertical loads or horizontal thrusts among themselves (Binda et al. 2001). These building blocks generally have the configuration and size defined by the urban layout of the village.

Stone masonry is a traditional constructive typology that has been practiced for centuries all over the world. These type of constructions were erected both in urban and in rural areas. Typically, in rural areas, as the case of the historical centre of *San Pio delle*

*Camere*, stone masonry buildings are smaller in their overall size, but they also have a smaller percentage between the volume of openings and the overall volume of the building, being the quality of construction lower than the one observed in urban stone masonry buildings (Fonti et al. 2013).

In order to carry out the seismic vulnerability assessment of buildings typology, engineers need a certain survey accuracy level. It is obvious the more detailed the survey level is, the more reliable results are. In this sense, the University of Pisa has developed a detailed survey of building aggregates in the entire village, providing the required data for the studied carried out (Mannari et al. 2011). This report, the so-called Aggregate Form (in Italian *Scheda di Aggregato*), contains the main input information needed for further seismic vulnerability evaluation, such as the aggregate geometry, conservation state, damage survey, plan drawings, elevations and explanatory pictures, as suggested by the ReLUIS project (ReLUIS 2010).

## 4 The building aggregate case study

The selected case study is a building aggregate composed of six Structural Units (S.U.) designated from A to F, mainly used as residential buildings (see Figs. 1, 3). The urban delimitation of this row building aggregate, is given by the street layout, in this case represented by *Via del Protettore* from the north and a secondary street on the south. From the west side, the building aggregate is delimited by a flight of stairs providing the discontinuity between the row end structural unit S.U. F and the adjacent building. The building aggregate has a total plan area of 319.5 $m^2$ and a total volume of 4535 $m^3$. The wall thickness of structural units varies approximately between 0.50 and 1.10 meters, while heights range between 2.60 and 3.20 m. The north facade has two underground storeys, representing approximately 15.5 % of the total volume of the aggregate, accounting for higher stiffness when compared with the opposite facade. Moreover, openings, represent approximately 7 % of the total vertical surface (load bearing walls), are not distributed evenly and their sizes vary significantly.

Even though several experimental tests were carried in *L'Aquila* and in surrounding areas (Candela et al. 2011), there is no information relative to the existence of such tests carried in *San Pio delle Camere*. Moreover, as complete material descriptions of case studies are rarely available and realising its importance in numerical analyses, the mechanical properties of the materials found in this case study were chosen according to

**Fig. 1** South facade (**a**) and north facade, (**b**, **c**) of the modelled building aggregate located in *San Pio delle Camere*, Italy (Scheda di Aggregato 2010)

materials database provided by 3muri® software, which is in turn derived from the values suggested by the Italian Ministerial Decree 14/01/2008 (DM 2008) for different masonry typologies. Moreover, according to this code, the Confidence Factor, *FC*, equal to 1.35 was assigned, corresponding to a knowledge level for limited information, *LC1*, aggravating the pre-set strength related properties (marked in Table 1 with an asterisk) and leading to a more conservative analysis. The only information provided regarding the constituting materials were in the form of a few pictures and scarce description of materials and building solutions, which brought major difficulties on attributing the correct material typology. To each single typology presented in Table 1, are related the following mechanical properties: Young elasticity modulus, $E$; shear modulus, $G$; specific weight, $\gamma$; average compressive strength, $f_m$; average shear strength value, $\tau$; characteristic compressive strength, $f_k$, and the partial factor for material's properties, $\gamma_m$.

According to the pictures provided in the *Scheda di Aggregato* report, the authors considered this building aggregate as mainly constituted of inhomogeneous stone masonry. However, some parts were constructed resourcing to other materials, which added some geometric discontinuity (openings and floor levels) and raised some structural complexity to the model. In fact, while structural units S.U. C, S.U. D, S.U. E and S.U. F are mainly made of irregular and inhomogeneous stone masonry, structural units S.U. A and S.U. B have other different materials varying in height, whose identification was highly questionable. Thus, the authors decided to assign these materials with the following typologies and respective mechanical properties: reinforced render for irregular stone masonry fabric; lightweight cellular concrete blocks and reinforced concrete (see Table 1; Fig. 2).

The seismic sequence that struck *L'Aquila* province took place between October and December 2008, with several thousands of foreshocks and aftershocks, some of them with significant values on the Richter magnitude scale. However, the main shock (lasting 20 s) was recorded at 1:32:40 UTC on 6th April 2009, rating 5.8 on the Richter scale and 6.3 on the moment magnitude scale, $M_w$. The epicentre, having as coordinates Lat.42°34′76 N and Long.13°38′00E, was about 10 km west of the surface rupture, and the seismic shaking and ground subsidence was dominant mostly in between the epicentre and the surface of rupture, coinciding more or less with the morphology of the *Aterno* Valley (Salamon et al. 2010). The pattern and intensity of damage were also function of the local site, basin and directivity effects, as well as the lack or absence of anti-seismic devices or design of the built environment. The damage was mostly caused by ground shaking followed by a couple of surface rupture events and slope failures.

**Table 1** Mechanical properties of load bearing walls materials

| Materials | $E$ (N/mm$^2$) | $G$ (N/mm$^2$) | $\gamma$ (kN/m$^3$) | $f_m^*$ (N/cm$^2$) | $\tau^*$ (N/cm$^2$) | $f_k^*$ (N/cm$^2$) | $\gamma_m$ (–) |
|---|---|---|---|---|---|---|---|
| Irregular stone masonry | 690 | 230 | 20 | 100.0 | 2.0 | 210.0 | 3.0 |
| Lightweight cellular concrete blocks | 1400 | 350 | 12 | 111.1 | 7.0 | 77.8 | 3.0 |
| Reinforced concrete C16/20 | 24 | 11920 | 25 | 24.0 | 10.0 | 16.0 | 1.5 |
| Reinforcement render over masonry in irregular stone | 2175 | 725 | 20 | 185.2 | 3.7 | 129.6 | 3.0 |

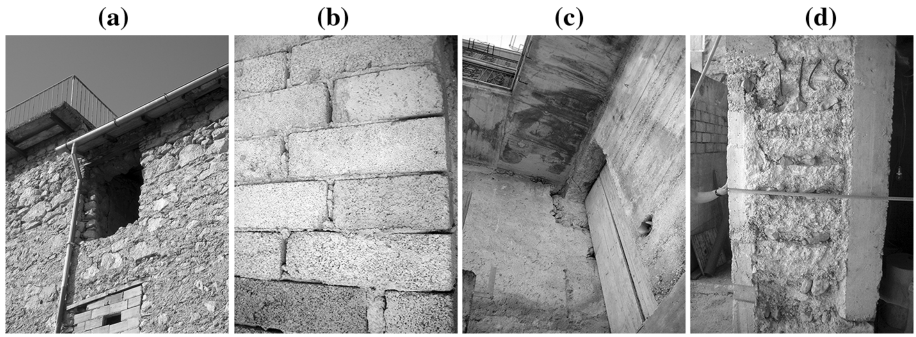


**Fig. 2** Different load bearing walls found in the assessed building aggregate: **a** irregular stone masonry; **b** lightweight cellular concrete blocks; **c** reinforced concrete and **d** reinforcement render over masonry in irregular stone

The damage verified in *San Pio delle Camere* was not as severe as in *L'Aquila* and other surrounding villages (Indirli et al. 2013; Formisano et al. 2010a; Formisano 2012), due to the soil quality (rocky soil), which reduced the amplification of seismic waves. The damage intensity on this village was evaluated in the Marcalli–Cancani–Sieberg scale as $I_{\mathrm{MCS}} =$ V–VI (Mannari et al. 2011).

## 5 Hybrid technique

The seismic vulnerability of the building aggregate was evaluated through a hybrid technique based on the CSM method. Thus, in order to estimate fragility curves and damage probability distributions, a correlation between the well-known macrosseismic methodology (Grünthal 1998) and the bilinear capacity curve (obtained through non-linear numerical analysis) was used.

The 3muri® software was the selected tool to perform pushover analysis on the building aggregate, enabling the assessment of its global seismic response. This software uses the Frame by the Macro-Elements (FME) method, in which macro-elements dimensions are a function of the global geometry of the aggregate, the dimension of the storeys, openings and the distances between openings (Ademović and Oliveira 2012; Marques et al. 2012). The formulation of masonry macro-elements emerged by observing the post-event effects in masonry structures. 3muri® assumes that structures can be efficiently represented as a combination of masonry panels constituted by spandrel beams and piers, subsequently represented by macro-elements with non-linear behaviour, connected by rigid nodes. This formulation reproduces the three principal in-plan collapse modes of masonry panels, the bending-rocking, shear-sliding and diagonal shear cracking, with a limited number of degrees of freedom, allowing representing the seismic response of complex masonry structures with a very limited computational demand. Figure 4 shows the resulting three-dimensional numerical view of the building aggregate and the differences between the original and simplified in-plan geometry.

The elastic horizontal response spectrum was defined according to required spectral parameters $a_g$, $F_0$ and $T_c$, attached in Table 1 of Annex B of the Italian Ministerial Decree 14/01/2008 (DM 2008), which are herein defined according to the site geographic coordinates of the aggregate building. These three parameter values ($a_g = 0.26$ g, $F_0 = 2.37$

and $T_c = 0.35$ s) have been estimated for a return period, $T_R$, equal to 475 years, considering the Life Safety limit state, ULS. To complete the response spectrum two additional factors were needed, the subsoil factor, $S_S$, and the topographic category factor, $S_T$, calculated as suggested on the NTC. The elastic response spectrum was converted in the ADRS (Acceleration–Displacement Response Spectrum) format (Chopra and Goel 1999), representing the spectral acceleration, $S_a$, versus the spectral displacement, $S_d$, for evaluating the seismic response of the case study, again following the Italian Ministerial Decree 14/01/2008 (DM 2008).

Pushover non-linear analyses were performed using 3muri®, again following the recommendations of the Ministerial Decree 14/01/2008 (DM 2008), which suggest that pushover analyses should be performed for both positive and negative orientations of the longitudinal and transversal earthquake directions, $U_x$ and $U_y$, respectively. Moreover, seismic loads should be represented by uniform pattern of lateral loads proportional both to mass and to the first vibration mode of the structure. Finally, the code requires that these analyses should realise accidental eccentricity of the centre of mass with respect to the rigidity centre automatically computed (5 % of the maximum planar distance perpendicular to the seismic action direction), making a total of twenty-four pushover curves. Furthermore, due to the structural complexity reflected by irregularity and heterogeneity of the model under analysis, some crosscutting assumptions were considered to understand the influence of some features over the global behaviour and modelling convergence of the building aggregate. Thus the authors assumed a mass weighted displacement at the third floor controlled by node, $N_{70}$, the lateral constraint effect induced on the north façade basement walls due to the uneven terrain real conditions (see Fig. 3) and also 3muri® default fixed wall-floor constraints. Hence, the most unfavourable analysis was obtained for longitudinal and transversal negative directions with a modal load distribution

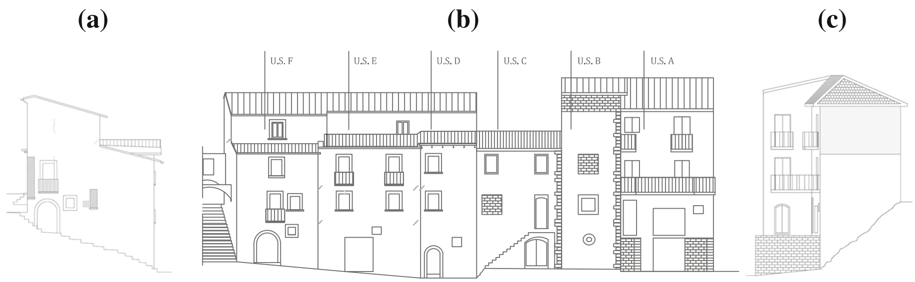


**Fig. 3** West elevation (**a**), south facade (**b**) and east elevation (**c**) of the case study building aggregate

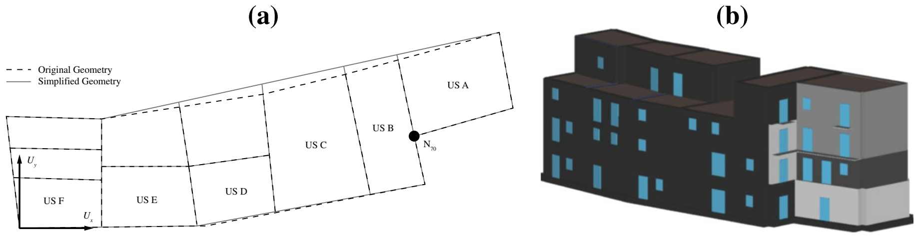


**Fig. 4** Original geometry versus the simplified geometry used in the 3muri® model (**a**) and the overview of the south facade of the modelled building aggregate

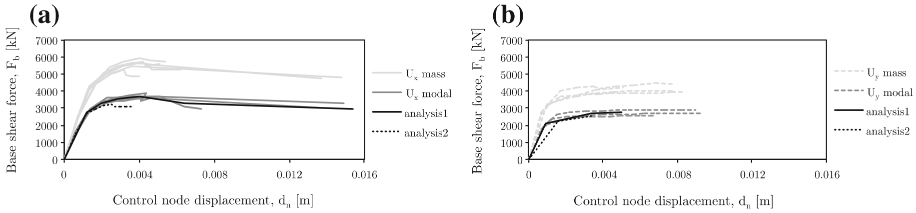


**Fig. 5** Pushover curves results highlighting *analysis 1* and *analysis 2:* **a** $U_x$ and **b** $U_y$ directions

considering no accidental eccentricity, which will be referred hereinafter as *analysis 1*. One other combination, *analysis 2*, was distinguished in the $U_x$ and $U_y$ positive direction for the same load pattern, but accounting for accidental eccentricity effects. Subsequently, the remaining pushover curves were grouped by load pattern type for each direction, referred hereinafter as $U_{i,mass}$ and $U_{i,modal}$, corresponding to mass and modal load distributions of direction $U_i$ (see Fig. 5).

In this way, Fig. 5 highlights the *analysis 1* and *analysis 2* pushover curves for both $U_x$ and $U_y$ directions, with the remaining $U_{i,mass}$ and $U_{i,modal}$ grouped analyses plotted on the background. From these results, it is possible to observe a base shear force value, $F_b$, in the transversal direction $U_y$ lower than the longitudinal direction $U_x$, which is explained by the ratio of resistant load bearing wall area, which is significantly lower along the $U_y$ direction. Moreover, base shear force values, $F_b$, vary between 3000 and 6000 kN for the $U_x$ direction. In the transversal direction $U_y$, $F_b$ varies between 2000 and 4000 kN, approximately. With respect to the control node ultimate displacements, $d_n$, these values ranged from 0.4 to 1.6 cm and from 0.4 to 1.0 cm for the $U_x$ and $U_y$ directions, respectively.

The observed base shear force values are quite high for traditional stone masonry structures. A simple relation between the total base shear force and gravity loads justifies this extremely high value. Such value is likely to be achieved due to the small ratio between the volume of openings and the total volume of walls. Moreover, the large thickness of masonry walls, some reaching 1.00 meter thick, and the short span between walls, increased the stiffness in this direction and, subsequently, the base shear force, $F_b$. Moreover, the modal load distribution analyses were estimated roughly 2000 kN below the uniform load distribution ones.

The main parameters achieved for the referred pushover analysis, shown in Table 2, resume both yielding and ultimate capacity, among other important output values, such as the minimum safety factor, $\alpha_u$, the mass participation factor, $\Gamma$, the yielding force of the

**Table 2** Overall results obtained through the application of the CSM method for pushover non-linear *analysis 1* and *analysis 2* carried out using 3muri®

| | $d_{max}$ (m) | $d_u$ (m) | $\alpha_u$ (–) | $\Gamma$ (–) | $T^*$ (s) | $F_y^*$ (kN) | $d_y^*$ (m) | $d_u^*$ (m) | $A_y$ (g) | $\mu$ (–) |
|---|---|---|---|---|---|---|---|---|---|---|
| *Analysis 1* | | | | | | | | | | |
| $-U_x$ | 0.0033 | 0.0050 | 1.24 | 0.65 | 0.12 | 3891 | 0.0017 | 0.0076 | 0.39 | 4.53 |
| $-U_y$ | 0.0062 | 0.0154 | 1.62 | 0.86 | 0.13 | 3781 | 0.0016 | 0.0179 | 0.45 | 10.86 |
| *Analysis 2* | | | | | | | | | | |
| $+U_x$ | 0.0065 | 0.0037 | 0.73 | 0.86 | 0.13 | 3590 | 0.0016 | 0.0043 | 0.36 | 2.69 |
| $+U_y$ | 0.0264 | 0.0046 | 0.26 | 1.08 | 0.26 | 1966 | 0.0026 | 0.0042 | 0.43 | 2.07 |

equivalent SDoF (single degree-of-freedom) system, $F_y^*$, the yielding and ultimate displacement of the equivalent SDoF system, $d_y^*$ and $d_u^*$, the yielding capacity of the SDoF system, $A_y$ and ductility coefficient, $\mu$. It is relevant to underline that the performance point values, $d_{max}$ (also known as structural demand displacement), is used to estimate fragility curves. Thus, for *analysis 1*, $d_{max}$ was evaluated as 0.33 cm for the longitudinal direction $U_x$ and as 0.62 cm for the transversal direction $U_y$. Moreover, the displacement capacity of the structure $d_u$ was equal to 0.50 cm and 1.54 cm for the $U_x$ and $U_y$ directions, respectively. The period, $T^*$, relative the equivalent Single Degree of Freedom system was evaluated as 0.12 and 0.13 s for the $U_x$ and $U_y$ directions, respectively, being in accordance with the previous results, since lower period means lower displacement values.

Once determined the spectral response, fragility curves were developed by calculating cumulative conditional probabilities of reaching or exceeding a given damage limit state (FEMA 2003). These damage limit states were defined for the "Unreinforced masonry bearing walls" typology, whereas to each damage limit states is associated a spectral displacement value related to the yielding and ultimate capacity, which in turn are related to the seismic action deformation response of the equivalent SDOF system, from the elastic behaviour range until reaching the collapse, corresponding to the previous values of $d_y^*$ and $d_u^*$, respectively.

Having defined the damage limit states, fragility curves were obtained according to the conditional probability $P[d_S|S_d]$ of reaching or exceeding a given damage state, $d_s$, for a determined spectral displacement $S_d$, according to the Eq. (1):

$$P[d_s|S_d] = \Phi\left[\frac{1}{\beta_{ds}}\ln\left(\frac{S_d}{S_{d\,ds}}\right)\right] \tag{1}$$

where $\Phi$ is the standard normal cumulative distribution function, $\overline{S_{d_{ds}}}$ is the median value of spectral displacement at which the building reaches the threshold of damage state, $d_s$, and $\beta_{ds}$ is standard deviation of the natural logarithm of spectral displacement for a damage state $d_s$. (see Table 3).

This limit damage state, $d_s$, considering the nominal mean values of spectral displacement are given by the expressions in following Eq. (2), according to FEMA (2003). From Fig. 6 it is possible to compare the fragility curves corresponding to *analysis 1*, obtained to the $U_x$ and $U_y$ directions, whereas damage grade $D_{k2}$ prevails in both directions.

$$\begin{array}{ll} (\text{Slight damage}) & S_{d_1}^{NV} = 0.7D_y \\ (\text{Moderate damage}) & S_{d_2}^{NV} = 1.5D_y \\ (\text{Severe damage}) & S_{d_3}^{NV} = 0.25\left(D_u + D_y\right) \\ (\text{Extremely severe damage or collapse}) & S_{d_4}^{NV} = D_u \end{array} \tag{2}$$

Once obtained the fragility curves, further damage probability histograms were obtained for different damage states, using the following Eq. (3) for the spectral displacement value, $S_d^*$, corresponding to the performance point of the structure (indicated in Fig. 6):

**Table 3** *Analysis 1* fragility curves input values

| | | Damage state, $d_s$ | | | | $\beta_{ds}$ (–) |
|---|---|---|---|---|---|---|
| | | $d_1$ | $d_2$ | $d_3$ | $d_4$ | |
| $U_x$ | $\overline{S_{d_{ds}}}$ | 0.00119 | 0.00255 | 0.00465 | 0.00760 | 0.60428 |
| $U_y$ | $\overline{S_{d_{ds}}}$ | 0.00112 | 0.0024 | 0.00975 | 0.01790 | 0.95403 |

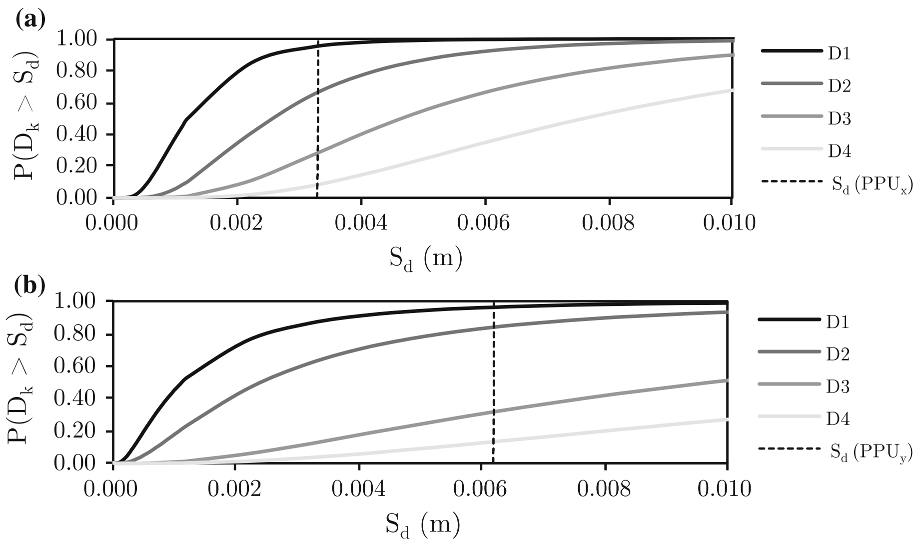


**Fig. 6** *Analysis 1* fragility curves corresponding to the **a** $U_x$ and **b** $U_y$ directions, with the respective performance point spectral displacements highlighted by the *dashed line*

$$P\left[d_{sk}|S_d^*\right] = \Phi\left[\frac{1}{\beta_{ds}}\ln\left(\frac{S_d^*}{\overline{S}_{d\,dsk}}\right)\right] \tag{3}$$

where $k$ can assume the values corresponding to each damage state ($k = 1$ up to 4). The damage discrete distribution function was obtained by the following Eq. (4), whereas $D_k$ represents each structural damage limit state defined according the EMS-98 scale (Grünthal 1998; Giovinazzi 2005) and $k$ varies from 1 up to 3.

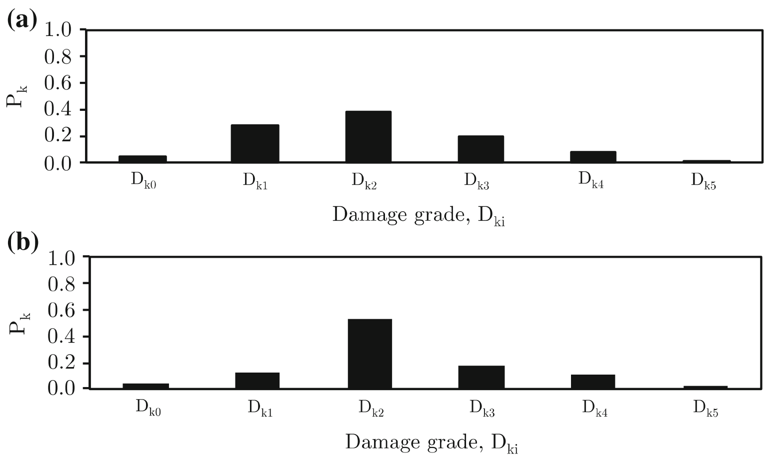


**Fig. 7** *Analysis 1* damage discrete distribution for the **a** $U_x$ and **b** $U_y$ directions

$$\begin{aligned} P(D_0) &= 1 - P\left[d_{s1}|S_d^*\right] \\ P(D_k) &= P\left[d_{s_k}|S_d^*\right] - P\left[d_{s_{k+1}}|S_d^*\right] \\ P(D_5) &= P\left[d_{s_5}|S_d^*\right] \end{aligned} \tag{4}$$

Figure 7 shows the corresponding damage discrete distribution, which again resulted centred around the damage grade $D_{k2}$, with a damage probability of 38.0 and 52.3 % for the $U_x$ and $U_y$ directions, respectively. In fact, this difference between both planar directions is associated to the value of $d_{max}$, which is larger in the transversal direction $U_y$, resulting slightly higher damage probabilities when compared to the longitudinal direction $U_x$. Later on, the presented damage distribution for *analysis 1* will be compared with the ones obtained through indirect techniques.

## 6 Indirect technique: individual buildings assessment

Within indirect techniques two different vulnerability index based methodologies were used on the seismic vulnerability assessment of individual buildings regarding the assessment of the seismic vulnerability of individual buildings were applied, adapted from the original GNDT II level methodology (GNDT-SSN 1994). Moreover, Benedetti and Petrini (1984) developed vulnerability functions, by means of a deterministic correlation between the seismic action and the damage level. This binomial relationship was reached through extensive and detailed information and post-seismic observation of damaged masonry buildings in the Italian territory. The characteristics that govern the seismic

**Table 4** Vulnerability index methodology proposed by Vicente (2008)

| Parameter | | Class $C_{vi}$ | | | | Weight | Relative weight over $I_v$ |
|---|---|---|---|---|---|---|---|
| | | A | B | C | D | $p_i$ | |
| *1. Structural building system* | | | | | | | |
| P1 | Type of resisting system | 0 | 5 | 20 | 50 | 0.75 | |
| P2 | Quality of resisting system | 0 | 5 | 20 | 50 | 1.00 | |
| P3 | Conventional strength | 0 | 5 | 20 | 50 | 1.50 | 46/100 |
| P4 | Maximum distance between walls | 0 | 5 | 20 | 50 | 0.50 | |
| P5 | Number of floors | 0 | 5 | 20 | 50 | 1.50 | |
| P6 | Location and soil conditions | 0 | 5 | 20 | 50 | 0.75 | |
| *2. Irregularities and interactions* | | | | | | | |
| P7 | Aggregate position and interaction | 0 | 5 | 20 | 50 | 1.50 | |
| P8 | Plan configuration | 0 | 5 | 20 | 50 | 0.75 | 27/100 |
| P9 | Height regularity | 0 | 5 | 20 | 50 | 0.75 | |
| *3. Floor slabs and roofs* | | | | | | | |
| P10 | Facade wall openings and alignments | 0 | 5 | 20 | 50 | 0.50 | |
| P11 | Horizontal diaphragms | 0 | 5 | 20 | 50 | 1.00 | 15/100 |
| P12 | Roofing system | 0 | 5 | 20 | 50 | 1.00 | |
| *4. Conservation status and other elements* | | | | | | | |
| P13 | Fragilities and conservation status | 0 | 5 | 20 | 50 | 1.00 | 12/100 |
| P14 | Non-structural elements | 0 | 5 | 20 | 50 | 0.50 | |

behaviour of masonry old buildings are treated as parameters, which must be evaluated in order to assess the vulnerability index value.

Firstly, it was used the vulnerability index methodology proposed by Vicente (2008) and described in Table 4, which has been used on large-scale assessment of some Portuguese historical centres, such as Coimbra and Seixal (Ferreira et al. 2013). This method the is applied through the calculation of a vulnerability index, $I_V^*$, which varies between 0 and 650, and is obtained from the weighted sum of fourteen parameters, which in turn are classified into four vulnerability classes, $C_{Vi}$, from $A$ to $D$. These parameters evaluate fourteen different aspects considered essential to assess their seismic global behaviour, weighted by means of the $p_i$ values, ranging from 0.5 up to 1.5, representing the lower or higher importance in the building's vulnerability. Thus, $I_V$, results as the normalised value of $I_V^*$, varying from 0 to 100. Once calculated this vulnerability index, $I_V$, damage distributions were estimated for different seismic intensities represented through the European Macroseismic Scale (Grünthal 1998). Although being a limited assumption for buildings aggregates with very inhomogeneous structural units, the mean vulnerability index value, $I_{Vm}$, was calculated as the average of the $I_V$ values estimated for each structural unit, only as a further confrontation indicator between hybrid and indirect techniques.

Adopting the principles of a macroseismic methodology, it was possible to obtain the mean damage grade $\mu_D$ [see the following Eqs. (5) and (6)] for different macroseismic intensities, $I_{\text{EMS-98}}$. Once defined the vulnerability index, $V$, for the $I_{Vm}$ mean value, varying between 0 and 1, and the ductility coefficient $Q$ (assumed equal to 2.3 for this type of masonry buildings), which represents the ratio between damage growth and the seismic intensity, mean damage grade curves can be obtained (Vicente 2008; Lagomarsino and Giovinazzi 2006; Giovinazzi 2005).

$$\mu_D = 2.5\left[1 + \tanh\left(\frac{I + 6.25V - 13.1}{Q}\right)\right]; \quad 0 \le \mu_D \le 5 \tag{5}$$

$$V = 0.58 + 0.0064 I_V \tag{6}$$

With this mean damage grade, $\mu_D$, it is possible to estimate damage distributions through histograms for different intensities $I_{\text{EMS-98}}$. In this study, binomial and beta probability functions were used to perform these histograms of damage distribution (Spence et al. 2003).

Later on, Formisano et al. (2010b) developed a similar vulnerability index based methodology, but this time accounting for the evaluation of fifteen parameters, wherein the last five regard the influence of adjacent buildings over the behaviour of each individual structural unit. Scores and weights of these additional parameters were evaluated through numerical analyses performed with the 3muri® software (Formisano et al. 2011). Similarly to the before mentioned methodology, a vulnerability index, $I_V$, was estimated for each structural unit according to the evaluation of referred fifteen parameters.

**Table 5** Vulnerability index values $I_{v,vic}$ and $I_{v,for}$, calculated for each structural unit

| | *S.U. F* | *S.U. E* | *S.U. D* | *S.U. C* | *S.U. B* | *S.U. A* |
|---|---|---|---|---|---|---|
| $I_{V,vic}$ | 60.4 | 39.0 | 39.0 | 33.3 | 23.8 | 36.5 |
| $I_{V,for}$ | 57.3 | 38.8 | 36.9 | 28.7 | 15.1 | 31.1 |

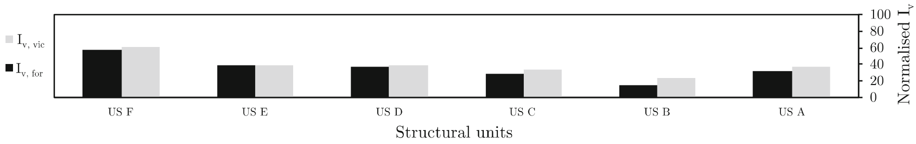


**Fig. 8** Comparison between both vulnerability index methodologies for individual buildings assessment, in terms of the attained normalised vulnerability index values $I_{v,vic}$ and $I_{v,for}$

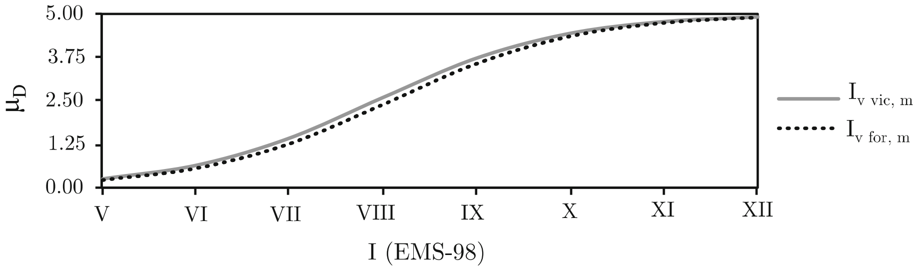


**Fig. 9** Vulnerability curves representing the mean damage grade $\mu_D$ for different intensities $I_{\text{EMS-98}}$, estimated for mean vulnerability index values of $I_{Vvic,\text{m}}$ and $I_{Vfor,m}$

Table 5 and Fig. 8 presents the differences between the vulnerability index values obtained from Vicente's ($I_{V,vic}$) and Formisano's ($I_{V,for}$) methodologies. Moreover, normalised vulnerability index mean values, $I_{Vm}$, were calculated in order to compare both approaches. The mean vulnerability index values $I_{Vvic,m}$ and $I_{Vfor,m}$ were evaluated as 38.7 and 34.6, respectively.

The comparison between the obtained vulnerability curves is shown in Fig. 9, where no relevant differences are noted, revealing a good approximation of these two

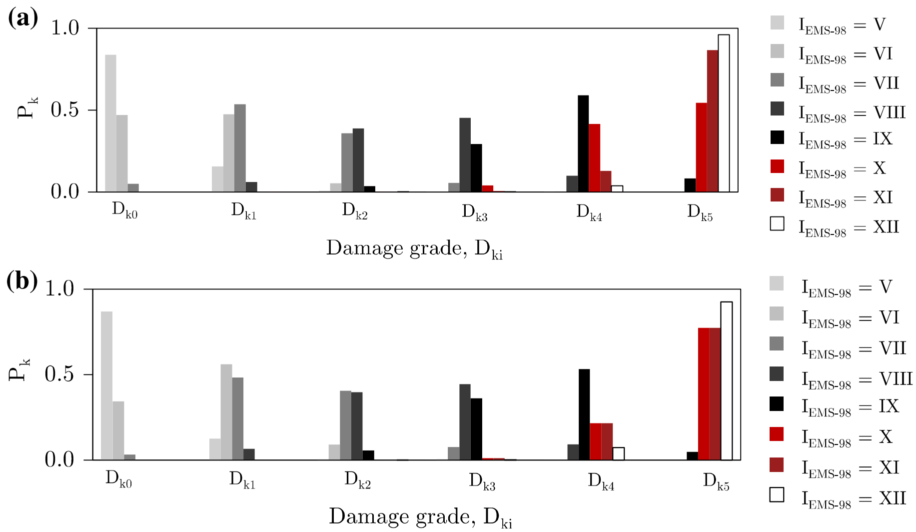


**Fig. 10** Damage distribution related to the mean damage grade $\mu_D$ for different seismic EMS-98 intensities, estimated for mean vulnerability index values of $I_{Vvic,\text{m}}$ (**a**) and $I_{Vfor,m}$ (**b**)

methodologies. Moreover, Fig. 10 compares damage distributions for different seismic intensities $I_{\text{EMS-98}}$ in terms of the mean damage grade $\mu_D$. These histograms of damage distribution, obtained for the vulnerability index methodologies, are defined through a beta distribution function developed by Bernardini et al. (2007), considering a parameter $t$, equal to 12.0, which is responsible to induce a low dispersion level on this beta distribution function (Vicente 2008). In general these damage distributions present higher differences for $I_{\text{EMS-98}}$ = VII, VIII and IX, in which Formisano's methodology show lower probabilities of damage.

## 7 Indirect technique: buildings in aggregate assessment

As the seismic vulnerability assessment of building aggregates is becoming a widely recognised topic, since the interactions between adjacent buildings should not be despised, it urges the development and validation of simplified methodologies exclusively directed for building aggregates. Hence, in this study, it was applied a vulnerability index based methodology developed by Vicente (2008) for this purpose. Similarly to the previously mentioned indirect techniques (from Sect. 6), this building aggregate vulnerability index value, $I^*_{V,a}$, varying between 0 and 225, is calculated as the weighted sum of five parameters related to the same four classes, $C_{Vi}$, of growing vulnerability (from $A$ to $D$). Again, each parameter evaluates an aspect regarding the seismic response of the building aggregate, through detailed analysis of several intrinsic properties of the structure. Subsequently, for each one of these parameters a weight $p_i$ is assigned, varying between 0.5 and 1.75, depending on the importance considered for each parameter. Finally, the building aggregate normalised vulnerability index value, $I_{V,a}$, is obtained from previous one, varying this way in between 0 and 100.

The $I_{V,a}$ value estimated for the building aggregate under analysis was 38.3. On one hand this value is very close to 38.7, from Vicente's mean vulnerability index, $I_{Vvic,m}$. On the other hand, $I_{V,a}$ differs approximately 10 % when compared to the 34.6 from the mean vulnerability index value, $I_{Vfor,m}$ (Table 6).

**Table 6** Seismic vulnerability assessment methodology for building aggregates, parameters and weights (Vicente, 2008; Ferreira et al. 2012)

| Parameter | | Class $C_{vi}$ | | | | Weight | Relative weight over $I^*_{v,a}$ |
|---|---|---|---|---|---|---|---|
| | | A | B | C | D | $p_i$ | |
| *1. Geometry* | | | | | | | |
| P1 | Quality and heterogeneity of masonry | 0 | 5 | 20 | 50 | 1.75 | 39/100 |
| *2. Irregularities* | | | | | | | |
| P2 | Openings misalignments | 0 | 5 | 20 | 50 | 0.50 | |
| P3 | Height irregularity | 0 | 5 | 20 | 50 | 0.75 | 44/100 |
| P4 | Plan configuration | 0 | 5 | 20 | 50 | 0.75 | |
| *3. Location and soil conditions* | | | | | | | |
| P5 | Location and soil quality | 0 | 5 | 20 | 50 | 0.75 | 17/100 |

## 8 Comparison between hybrid and indirect methodologies

The correlation between the EMS-98 scale and the peak ground acceleration value, PGA, is defined by the following Eq. (7), developed by Lagomarsino and Giovinazzi, which allows for the comparison between the damage distribution of both hybrid and indirect techniques (Giovinazzi and Lagomarsino 2006):

$$a_g = C_1 C_2^{(I-5)} \tag{7}$$

where $a_g$ is the peak ground acceleration in g, $I$ is the macroseismic intensity, $I_{\text{EMS-98}}$, $c_1$ is the coefficient which defines the PGA value for a default intensity and $c_2$ defines the slope of the correlation curve. As shown in Table 7, three different correlation laws developed by Guagenti-Petrini, Margottini and Murphy-O'Brien, were used to estimate the corresponding intensity $I$, for a peak ground acceleration value, $a_g$, equal to 0.255 g, for the examined site (Guagenti and Petrini 1989; Margottini et al. 1992; Murphy and O'Brien 1977). On one hand, for this PGA value and according to Guagenti-Petrini correlation law, the intensity $I_{\text{EMS-98}} =$ VIII was obtained. On the other hand, using the correlations proposed by Margottini and Murphy-O'Brien, the same PGA has led to an intensity $I_{\text{EMS-98}} =$ IX.

Figure 11 resumes the damage distributions for all the applied techniques, considering an equivalent $I_{\text{EMS-98}}$ based on the same PGA value used to perform the pushover analyses. Facing $I_{Vvic,m}$ and $I_{Vfor,m}$ damage distributions, it was observed a maximum deviation in

**Table 7** Values of $c_1$ and $c_2$ for $I_{\text{EMS-98}}$ – PGA correlation laws according to different authors

| Correlation law | $c_1$ | $c_2$ | $I_{\text{EMS-98}}$ |
|---|---|---|---|
| Guagenti-Petrini | 0.03 | 2.05 | VIII |
| Margottini | 0.04 | 1.65 | IX |
| Murphy-O'Brien | 0.03 | 1.75 | IX |

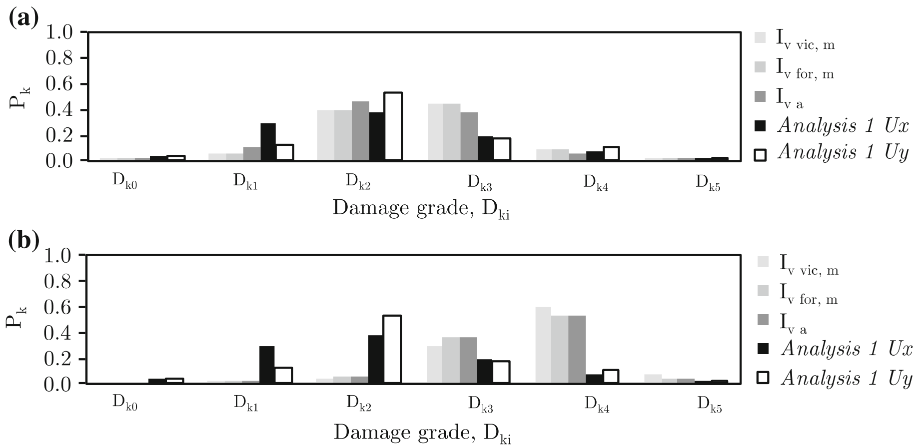


**Fig. 11** Damage distributions comparison between indirect and hybrid techniques for intensities: **a** $I_{\text{EMS-98}} =$ VIII and **b** $I_{\text{EMS-98}} =$ IX

$D_{k3}$ equal to 7.3 and 7.4 %, for $I_{EMS\text{-}98}$ = VIII and $I_{EMS\text{-}98}$ = IX, respectively. When comparing $I_{Vvic,\ m}$ with $I_{V,a}$ these difference are substantially reduced to 1.1 % for $I_{EMS\text{-}98}$ = VIII. However, when comparing $I_{Vvic,m}$ to *analysis 1* distributions, differences resulted more noticeable, since they have reached 25.1 and 51.8 % for the $U_x$ direction and 26.8 and 48.8 % for the transversal direction $U_y$. When compared to $I_{Vvic,m}$, generally smaller deviations were. For $I_{EMS\text{-}98}$ = VIII the maximum deviation value of 6.4 % was found compared to $I_{V,a}$. The expected deviations for $I_{EMS\text{-}98}$ = IX was higher, going against the observed trend. The comparison between $I_{Vfor,m}$ and the longitudinal direction of *analysis 1* reached the largest difference of 18.5 and 45.6 % for $I_{EMS\text{-}98}$ = VIII, whereas for $I_{EMS\text{-}98}$ = IX the maximum difference was 19.5 and 46.4 %, respectively. Finally, comparing $I_{V,a}$ for both directions of *analysis 1* distributions, it was registered a maximum deviation of 24.2 and 46.0 % in the $U_x$ direction, while in the $U_y$ these differences were 25.9 and 46.6 %, respectively.

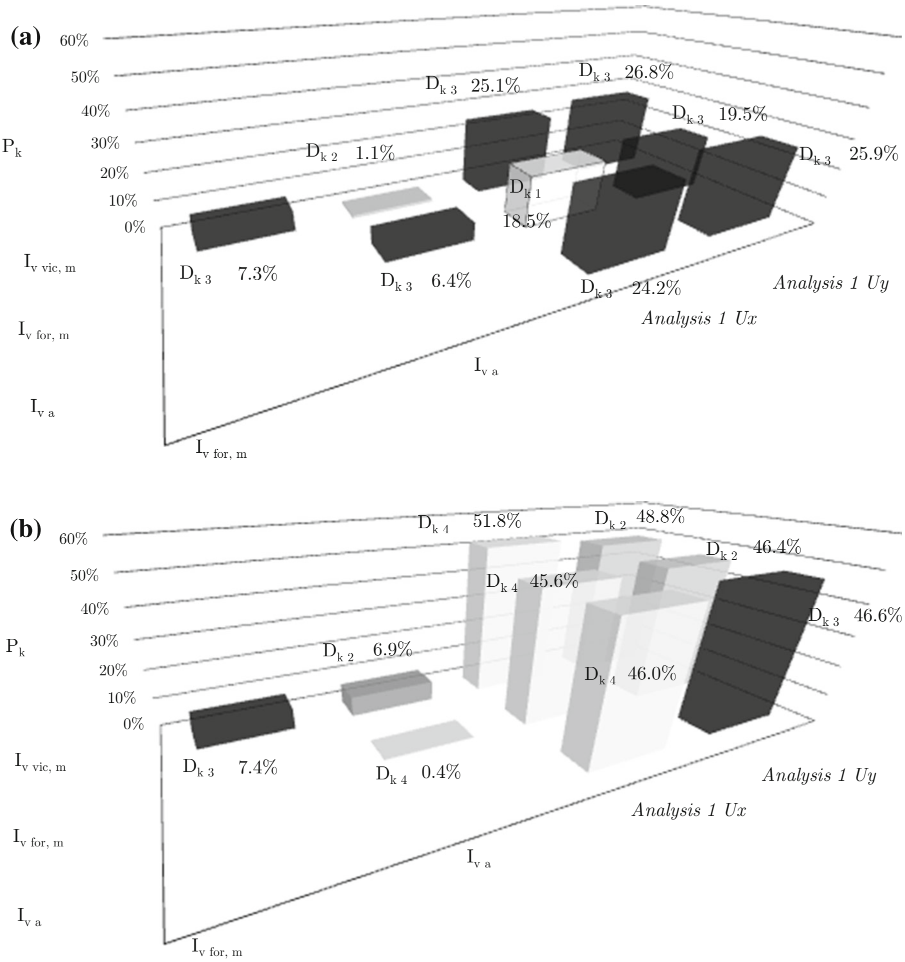


**Fig. 12** Damage grade $D_{Ki}$ corresponding to the maximum deviation value among damage distribution percentage for all methodologies for **a** $I_{EMS\text{-}98}$ = VIII and **b** $I_{EMS\text{-}98}$ = IX

Moreover, the following Fig. 12 shows the maximum deviation ratio of each corresponding damage grade, $D_{ki}$, for both intensities $I_{\text{EMS-98}} = \text{VIII}$ and $I_{\text{EMS-98}} = \text{IX}$. From comparing the vulnerability indexes based on different methodologies for an earthquake with intensity $I_{\text{EMS-98}} = \text{VIII}$, better approximations were found between the $I_{V,a}$ and $I_{Vvic,m}$, in which the most significant difference among the corresponding damage distributions showed a maximum value of 1.1 % for damage grade $D_{k1}$. The same comparison, but for a $I_{\text{EMS-98}} = \text{IX}$, have evidenced the $I_{Vfor,m}$ has the best approximation to $I_{V,a}$, with maximum deviation of 0.4 % for damage grade $D_{k4}$. Finally, comparing these last methodologies to the ones derived from the numerical analysis, it is possible to observe larger disparities on both macroseismic intensities, being this discrepancy even higher for $I_{\text{EMS-98}} = \text{IX}$.

## 9 Final comments

Building aggregates result as a middle term scale class of buildings whose optimal assessment should embrace numerical analysis for a more detailed investigation, always depending on the objective of the project in hands. The accuracy in the outcomes obtained through non-linear static analysis was found clearly influenced by the input parameters, such as the mechanical and geometrical properties of the structure. Therefore, the accuracy of the structural survey and inspection report provided is entirely reflected over the obtained results. In this study, while in-plan irregularities were successfully overcome, causing no numerical issues, in-height irregularities were more problematic, since they might have affected nodal displacements, hindering the safety verification and the analysis convergence. The results obtained distinguished the transversal direction, $U_y$, as the most vulnerable one, which is coherent with the observed damage verified in the in situ inspection, in which transversal walls were significantly more damaged than longitudinal walls. The lower node displacement values of the pushover analysis were a consequence of the effort in representing the behaviour of the slope between facades, through modifying the lateral supporting conditions of the model. This assumption was found too conservative and it might be related with inconsistencies regarding the generated mesh of the model. As a general comment, it is sensible to affirm that the damage distribution predicted by pushover curves are somehow assimilated to real damage distribution observed in the building aggregate, both in terms of extension and failures modes.

Indirect techniques were carried out to compare it with hybrid and more robust techniques. With respect to the individual structural assessment, the methodology proposed by Vicente showed slight differences in excess on the vulnerability index, when compared to the one developed by Formisano et al. (2011). Even though, both methodologies show highest vulnerability index values for structural units S.U. F, S.U. E and S.U. D, providing a good agreement between these results, with deviations below 5.5 %. On the contrary, it was found important deviations between these two methodologies for structural units S.U. A, S.U. B and S.U. C, which identifies the parameters relative to masonry material heterogeneity as the most different between both methodologies. Moreover, with respect to row end buildings S.U. A and S.U. F, higher vulnerability index values were expected, in agreement with the later studies conclusions regarding building aggregates vulnerability assessment. Mean vulnerability index values were estimated in order to construct a prediction of the building aggregate seismic vulnerability suitable to be compared with the building aggregate vulnerability index formulation proposed by Vicente. Therefore, on the one hand, the vulnerability index methodology designed to assess building aggregates approximates very accurately the mean vulnerability index values of Vicente's methodology. On the other hand, both vulnerability index formulations of Vicente and Formisano come quite closer for cases of regular buildings.

The conversion of the hybrid technique using the EMS-98 macroseismic scale was found to be a reasonable way of establishing comparisons with indirect techniques. Thus, it was possible to conclude that for a seismic intensity $I_{EMS\text{-}98} = \text{VIII}$, indirect techniques were found more representative of the real damage distribution in the building aggregate, from which the aggregate vulnerability index methodology has shown as the less conservative of the three vulnerability index methodologies. With respect to intensity $I_{EMS\text{-}98} = \text{IX}$, indirect techniques revealed to be too conservative, while, on the contrary, hybrid techniques failed this approximation by default. These comparisons between hybrid and indirect techniques were found to be somehow inaccurate for extreme macroseismic intensities and very similar for moderate ones. It was evident that data accuracy has severe implications on numerical analysis outputs, which can lead to unreliable results and interpretations. These computational analyses should be compared to quick vulnerability assessment methods in order to detect possible problems on numerical model environments. To avoid this, scientists should be aware and conscious about the knowledge level and survey quality, related to a generic study, assuring that all the required data is available, in order to achieve reliable results. When this required knowledge level is poor, or less satisfactory, it is preferable to conduct analysis through more simplified methodologies, which are proven to give satisfactory estimations for both damage and seismic vulnerability assessment of either individual buildings or building aggregates. This way, indirect techniques are also recommended as first assessment tool, in order to preview and prioritise intervention strategies for reducing the seismic vulnerability of the building aggregate. Afterwards, numerical analysis shall be used as a complement of indirect techniques assessment, for a more detailed examination of the structure and its behaviour when subjected to a seismic action, contributing for the designing of more adequate and efficient retrofitting interventions.

**Acknowledgments** The authors would like to acknowledge to Eng. Davide Seni of the S.T.A. DATA company for giving the license to work with 3muri® and Dr. Serena Cattari for the useful suggestions on the use of the program. Lastly, a sincere acknowledge to Prof. Mauro Sassu, who provided drawings and information on the case study.

## References

Ademović N, Oliveira DV (2012) Seismic assessment of a typical masonry residential building in Bosnia Herzegovina. In: Proceeding of the 15th world conference of earthquake engineering—WCEE, Lisbon, Portugal

Benedetti D, Petrini V (1984) Sulla Vulnerabilità Sismica degli Edifici in Muratura: proposta di un Metodo di Valutazione. L'industria Italiana delle Costruzioni 149(1):66–74 (In Italian)

Bernardini A, Giovinazzi S, Lagomarsino S, Parodi S (2007) Vulnerabilità e previsione di Danno a Scala Territoriale secondo una metodologia Macrosismica coerente con la Scala EMS-98. In: Proceedings of the 12th Italian conference on earthquake engineering, 10–14 June, Pisa, Italy (in Italian)

Binda L, Baronio G, Cardani G, Penazzi D, Tedeschi C, Tongini FR (2001) Il Progetto di Conservazione, 174–197. S. Pesenti, Alinea (in Italian)

Calvi GM, Pinho R, Magenes G, Bommer JJ, Restrepo-Vélez LF, Crowley H (2006) Development of seismic vulnerability assessment methodologies over the past 30 years. ISET J Earthq Technol 472(43):75–104

Candela M, Cattari S, Lagomarsino S, Fonti R, Pagliuca E (2011) Prove in situ per la Valutazione della Risposta nel Piano di un Pannello Murario in un Edificio a L'Aquila. In: Proceedings of the 14th Italian conference on earthquake engineering—ANIDIS. Italian National Association of Earthquake Engineering, Bari, Italy (in Italian)
Carocci CF, (2001) Guidelines for the safety and preservation of historical centres in seismic areas. In: Historical constructions, Guimarães, Portugal, pp 145–166
Chever L (2012) Use of seismic assessment methods for planning vulnerability reduction of existing building stock. In: Proceedings of the 15th world conference on earthquake engineering—WCEE, Lisbon, Portugal
Chopra AK, Goel RK (1999) Capacity-demand-diagram methods based on inelastic design spectrum. Earthq Spectra 15:637–656. doi:10.1193/1.1586065
DM (2008) Decreto Ministeriale 14/01/2008. Nuove Norme tecniche delle Costruzioni (in Italian)
Erdik M (2007) Earthquake disaster scenario prediction and loss modelling for urban areas. Lessloss report. Risk mitigation for earthquakes and landslides. IUSS Press, Pavia
FEMA (2003) Multi-hazard loss estimation methodology: earthquake model. Department of Homeland Security, FEMA, Washington, DC, Technical report
Ferreira TM, Vicente R, Varum H (2012) Vulnerability assessment of building aggregates: a macroseimic approach. In: Proceedings of the 15th world conference on earthquake engineering—WCEE, Lisbon, Portugal
Ferreira TM, Vicente R, Mendes da Silva JAR, Varum H, Costa A (2013) Seismic vulnerability assessment of historical urban centres: case study of the old city centre in Seixal, Portugal. Bull Earthq Eng 11:1753–1773. doi:10.1007/s10518-013-9447-2
Fonti R, Formisano A, Mazzolani FM (2013) Le strutture ad arco negli aggregati su pendio: un caso studio nel centro storico di San Pio delle Camere (AQ). In: Proceedings of the 15th Italian conference on earthquake engineering, Padova University Press, Padova, Italy (in Italian)
Formisano A (2012) Seismic behaviour and retrofitting of the Poggio Picenze Historical Centre damaged by the L'Aquila earthquake. In: Topping BHV, (ed) Proceedings of the eleventh international conference on computational structures technology, Civil-Comp Press, Stirlingshire, UK, Paper 199. doi:10.4203/ccp.99.199
Formisano A, Di Feo P, Grippa, MR, Florio G (2010a) L'Aquila earthquake: a survey in the historical centre of Castelvecchio Subequo. In: Proceedings of the COST action C26 final conference "urban habitat constructions under catastrophic events". Federico M. Mazzolani, Chair, Naples, 16–18 September 2010, CRC Press, Taylor & Francis Group, London, pp 371–376, ISBN: 978-0-415-60685-1
Formisano A, Mazzolani FM, Florio G, Landolfo R (2010b) A Quick Methodology for seismic vulnerability assessment of historical masonry aggregates. In: Proceedings of the COST action C26 final conference "urban habitat constructions under catastrophic events", Federico M. Mazzolani, Chair, Naples, 16–18 September 2010, CRC Press, Taylor & Francis Group, London, pp 577–582, ISBN: 978-0-415-60685-1
Formisano A, Florio G, Landolfo R, Mazzolani FM (2011) Numerical calibration of a simplified procedure for the seismic behaviour assessment of masonry building aggregates. In: Topping BHV, Tsompanakis Y (ed) Proceedings of the thirteenth international conference on civil, structural and environmental engineering computing, Civil-Comp Press, Stirlingshire, UK, Paper 172. doi:10.4203/ccp.96.172
Formisano A, Castaldo C, Mazzolani FM (2013) Non-linear analysis of masonry building compounds: a comparison of numerical and theoretical results. In: Topping BHV, Iványi P (eds) Proceedings of the fourteenth international conference on civil, structural and environmental engineering computing, Civil-Comp Press, Stirlingshire, UK, Paper 66. doi:10.4203/ccp.102.66
Freeman SA (1998) Development and use of capacity spectrum method. In: Proceedings of the 6th US NCEE conference on earthquake engineering, Seattle, Washington DC, USA
Giovinazzi S (2005) The vulnerability assessment and damage scenario in seismic risk analysis, PhD Thesis, University of Florence, Florence, Italy
Giovinazzi S, Lagomarsino S (2006) Damage assessment of current buildings at territorial scale: a mechanical model calibrated on a macroseismic vulnerability model. Genoa, Italy
GNDT-SSN (1994) Scheda di esposizione e vulnerabilità e di rilevamento danni di primo livello e secondo livello (muratura e cemento armato). Grupo Nazionale per la Difesa dai Terrmoti, Rome, Italy (in Italian)
Grünthal G (1998) European Macroseismic Scale 1998 (EMS-98), European Seismological Commission, Subcommission on Engineering Seismology, Working Group Macroseismic Scales 15:101
Guagenti E, Petrini V (1989) Il caso delle Vecchie Costruzioni: verso una nuova legge danni-intensità. In: Proceedings of the 12th Italian conference on earthquake engineering—ANIDIS. Italian National Association of Earthquake Engineering, Pisa, Italy (in Italian)

Indirli MS, Kouris LA, Formisano A, Borg RP, Mazzolani FM (2013) Seismic damage assessment of unreinforced masonry structures after the Abruzzo 2009 earthquake: the case study of the historical centers of L'Aquila and Castelvecchio. Int J Archit Herit 7:536–578. doi:10.1080/15583058.2011.654050

Lagomarsino S, Giovinazzi S (2006) Macroseismic and mechanical models for the vulnerability and damage assessment of current buildings. Bull Earthq Eng 4:415–443

Maio R (2013) Seismic vulnerability assessment of old stone masonry building aggregates. MSc Thesis, Civil Engineering Department of the University of Aveiro, Aveiro, Portugal

Mannari A, Scaramuzzino L, Stefanelli S et al (2011) Studi E Indagini Sul Rischio Sismico Del Centro Storico Di San Pio Delle Camere (AQ). Studi e Indagini sul Rischio Sismico del Centro Storico di San Pio delle Camere, 8800381:245 (in Italian)

Margottini C, Molin D, Narcisi B, Serva L (1992) Intensity versus ground motion: a new approach using Italian data. Eng Geol 33(1):45–58, ISSN 0013-7952. doi:10.1016/0013-7952(92)90034-V

Marques R, Vasconcelos G, Lourenço PB (2012) Pushover analysis of a modern aggregate of masonry building through macro-element modelling. In: Proceedings of the 15th international brick and block masonry conference, Florianopolis, Brazil

Mouroux P, Le Brun B (2006) Presentation of RISK-UE project. Bull Earthq Eng 4:323–339. doi:10.1007/s10518-006-9020-3

Murphy JR, O'Brien LJ (1977) The correlation of peak ground acceleration amplitude with seismic intensity and other physical parameters. Bull Seismol Soc Am 67(3):877–915

ReLUIS (2010) Linee Guida per il rilievo, l'analisi ed il progetto di interventi di riparazione e consolidamento sismico di edifici in muratura in aggregato, (draft version n.3). Developed by a joint working group: ReLUIS, Dipartimento Protezione Civile, Ufficio del Vice-Commissario Delegato per la Messa in Sicurezza dei Beni Culturali and Struttura Tecnica di Missione (in Italian)

Salamon A, Amit R, Baer G et al. (2010) The $M_w$ 6.3, 2009 L'Aquila earthquake, Central Italy: report of the GSI team visit to the affected area. Technical report, Jerusalem, Israel

Scheda di Aggregato (2010) Scheda di Aggregato No.8800378 of San Pio delle Camere, Italy. Technical report, University of Pisa, Pisa, Italy (in Italian)

Spence R, Bommer J, Re DDEL (2003) Comparing loss estimation with observed damage: a study of the 1999 Kocaeli Earthquake in Turkey. Bull Earthq Eng 1:83–113

Vicente R (2008) Estratégias e Metodologias para Intervenções de Reabilitação Urbana—Avaliação da Vulnerabilidade e do Risco Sísmico do Edificado da Baixa de Coimbra. PhD Thesis, Civil Engineering Department of the University of Aveiro, Aveiro, Portugal (in Portuguese)